SUPPLEMENTAL FIGURES

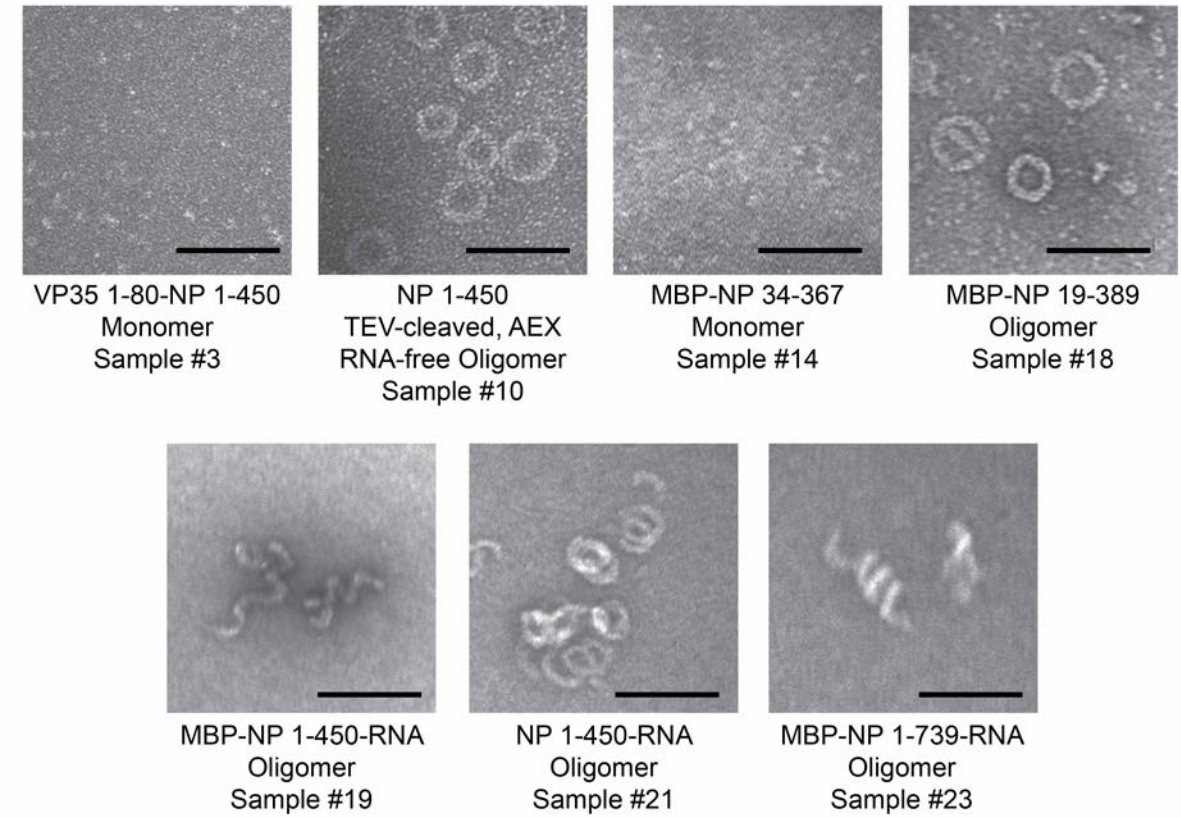

Supplemental Figure S1: Negative stain electron microscopy of Ebolavirus NP, Related to Table 1. Selected samples listed in Table 1 were imaged using negative stain electron microscopy. NP oligomers purified by affinity chromatography resemble short helices and rings. Scale bar is 100 nm.

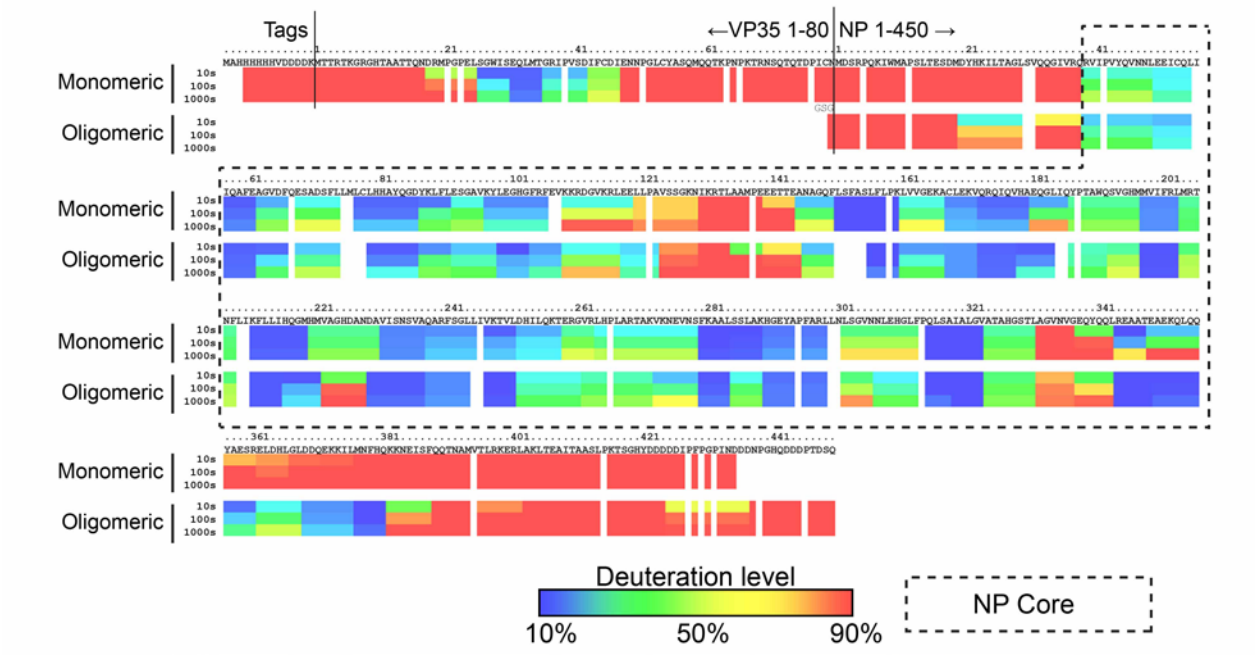

Supplemental Figure S2: Hydrogen/deuterium exchange mass spectrometry of EBOV NP N-terminal domain, Related to Figure 2. Monomeric RNA-free NP is the RNA-free VP35 1-80–NP 1-450 fusion protein (Table 1, sample 3). The regions corresponding to purification tags and VP35 are indicated. Oligomeric NP is the RNA-free NP N-terminal domain (1-450) produced by removing bound VP35 peptide and allowing *in vitro* oligomerization (Table 1, sample 10). The amount of deuteration at each amino acid position is indicated by the color scale shown. The NP core, protected from solvent in the monomeric NP is in a dashed box. Amino acid numbering of the protein constructs corresponds to positions within each protein.

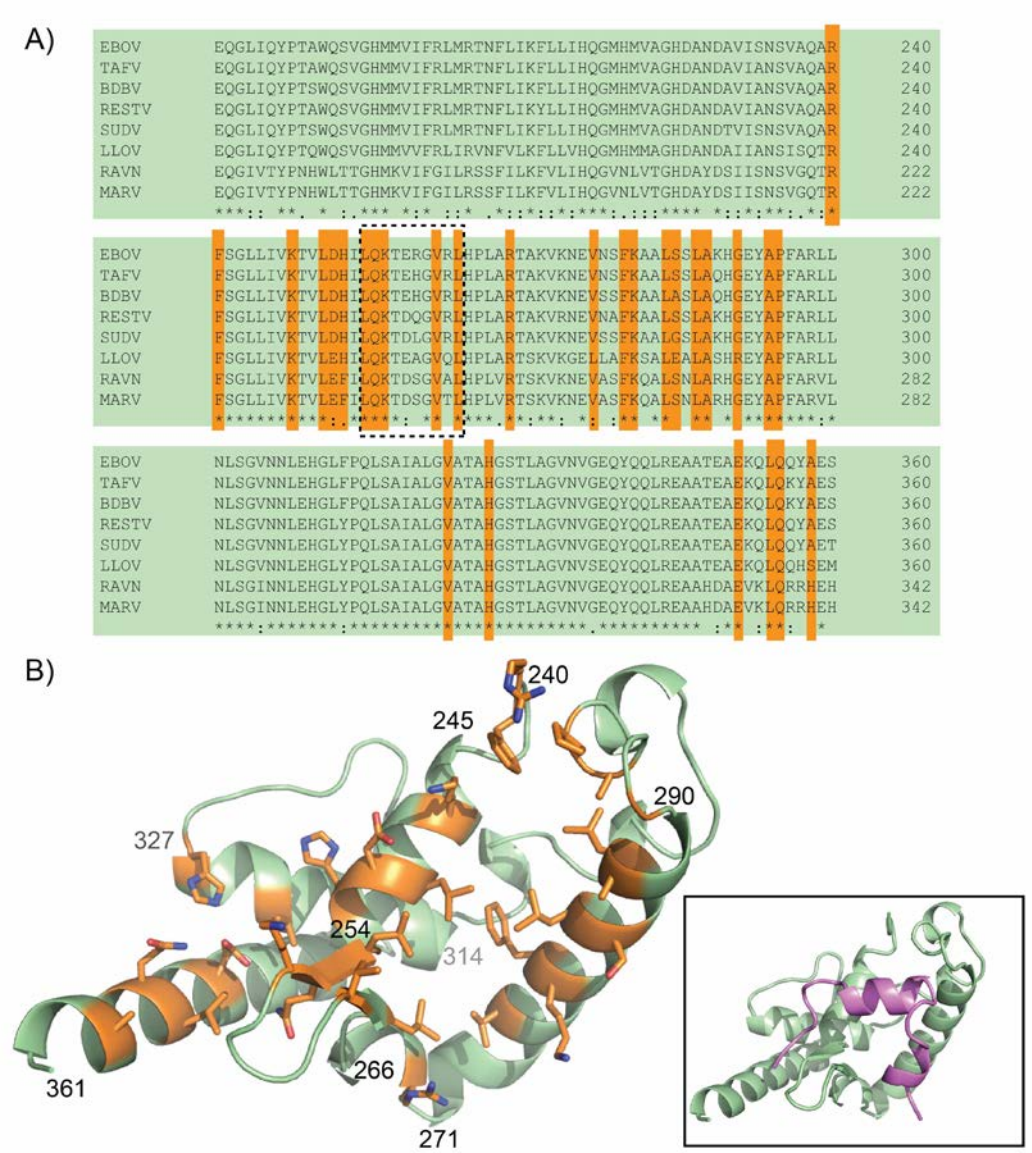

Supplemental Figure S3: VP35 interaction site on NP, Related to Figure 2. A) Sequence alignment of regions of filovirus NP interacting with the VP35 N-terminal peptide. Amino acids of EBOV NP that are within 4 Å of VP35 in the NP°-VP35 crystal structure are colored orange. The remaining portions of NP are colored green. The filovirus-unique β-hairpin is indicated with a dashed box. B) The EBOV NP C-terminal domain colored as in A) with the side chains of interacting amino acids shown as sticks. The inset shows the same view of the EBOV NP C-terminal domain (green) with the bound VP35 N-terminal peptide (purple).

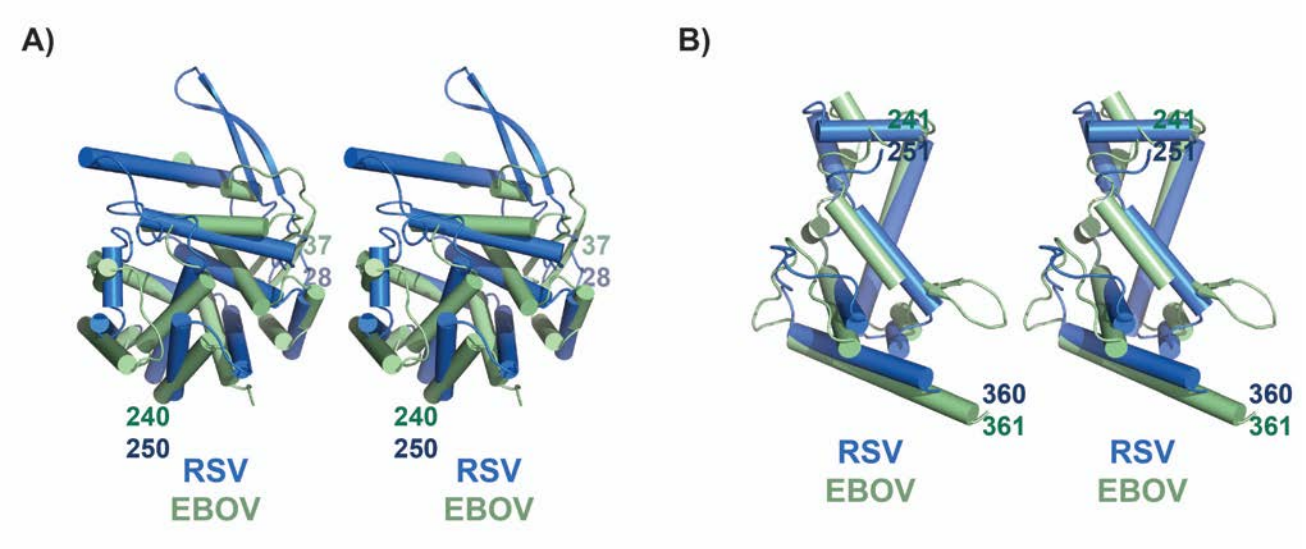

Supplemental Figure S4 : Structural homology of respiratory syncytial virus and Ebola virus nucleoprotein domains, Related to Figure 4. Superposition of A) the N-terminal domains and B) the C-terminal domains. Structures are shown as wall-eye stereo. The termini of the domains used for structural alignment are labeled.

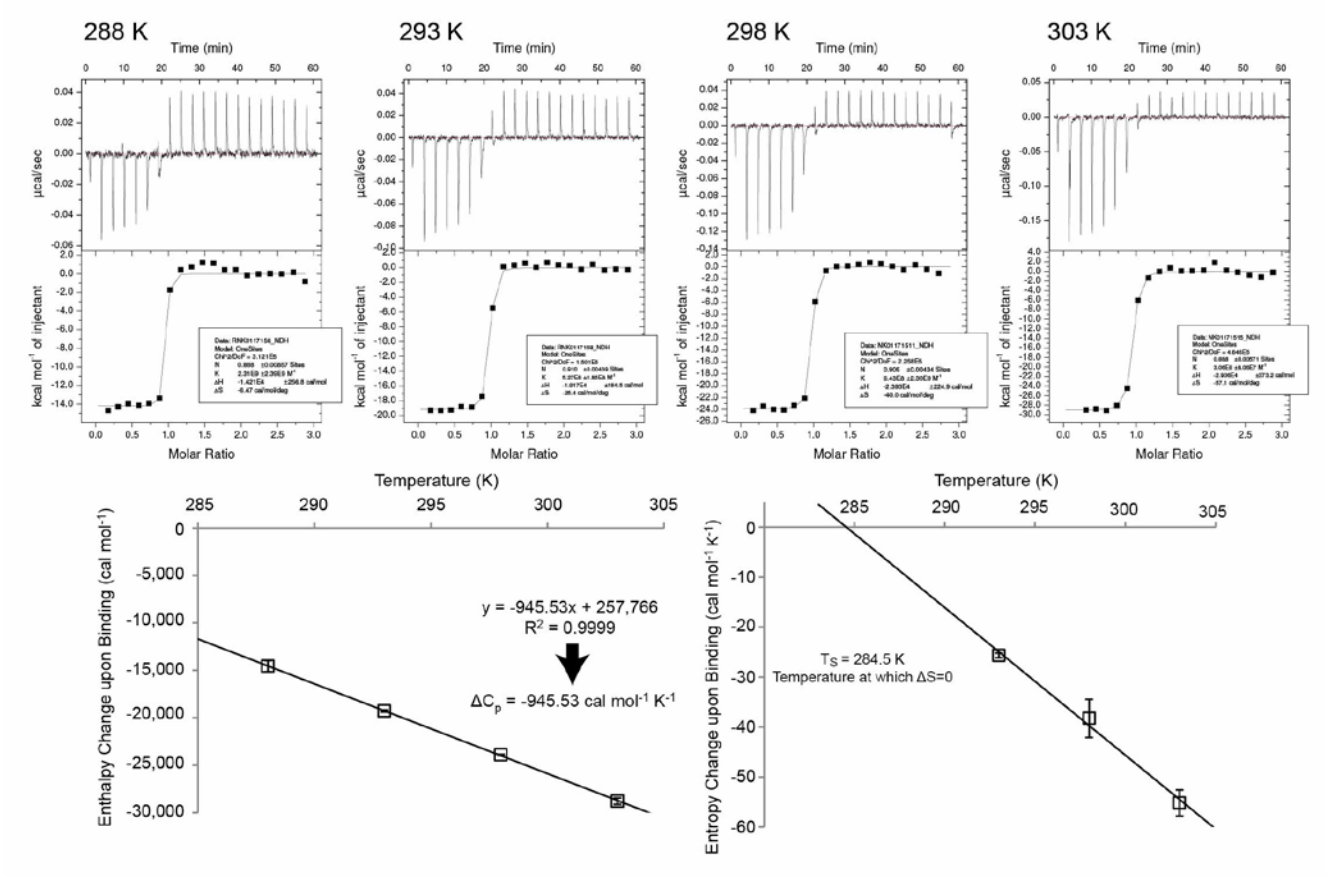

Supplemental Fig S5: Thermodynamics of the binding of EBOV VP35 1-80 to NP 34-367, Related to Figure 3. The binding of the VP35 1-80 peptide to the NP core (34-367) was assessed by isothermal titration calorimetry at different temperatures. The enthalpy (ΔH) and entropy (ΔS) were plotted with respect to temperature. The slope of the enthalpy vs. temperature data is equal to the heat capacity change upon binding (ΔC_p). The x-intercept of the entropy vs. temperature data reports the temperature at which the entropy is expected to be 0 cal mol^{-1} K^{-1} (T_S). Entropy data from the 288 K data point was not used due to the poor quality of fitting at this temperature.

	S-SAD	Native	Native
PDB	4ZTA	4ZTI	4ZTG
Data Collection			
Space group	$I2_12_12_1$	$P2_12_12_1$	$P22_12_1$
Unit cell			
a, b, c (Å)	91.1 93.0 114.9	94.9 95.0 112.1	33.3 92.4 133.6
α, β, γ (°)	90 90 90	90 90 90	90 90 90
No. of crystals	14	1	1
Wavelength (Å)	1.70004	1.0331	1.0332
Resolution (Å)	50-2.40 (2.49-2.40)	50-2.40 (2.54-2.40)	50-2.80 (2.95-2.80)
No. unique reflections	19,511 (2,012)	40,326 (6,357)	10,825 (1,486)
Completeness (%)	100 (99.9)	99.9 (99.8)	99.9 (96.8)
Anom. Completeness (%)	100 (99.9)	-	-
Multiplicity	172.7 (174.5)	7.4 (7.5)	6.3 (6.2)
Anom. Multiplicity	89.4 (88.6)	-	-
I/(σI)	43.7 (5.3)	8.2 (1.5)	12.9 (1.6)
R_{merge} (%)	15.8 (313.0)	16.2 (167.1)	8.4 (104.2)
$R_{p.i.m.}$ (%)	2.1 (23.6)	6.0 (60.7)	3.6 (44.9)
$CC_{1/2}$	100 (96.7)	99.3 (57.5)	99.8 (81.1)
Refinement			
Resolution (Å)	50-2.40 (2.46-2.40)	50-2.40 (2.46-2.40)	50-2.8 (2.87-2.80)
R_{work} (%)	20.4 (24.4)	19.3 (31.4)	25.9 (39.2)
R_{free} (%)	23.3 (28.0)	24.5 (31.9)	29.3 (41.0)
r.m.s.d			
Bonds (Å)	0.014	0.014	.012
Angles (°)	1.63	1.48	1.60
B-factors ($Å^2$)			
NP	80.9	64.8	91.5
VP35	80.1	73.4	95.6
Solvent	77.5	60.8	61.6
Wilson B-factor	67.3	62.3	79.5
Ramachandran (%)			
Favored	98.5	97.0	97.3
Outliers	0.0	0.0	0.0

Table S1. X-ray diffraction data collection and refinement statistics, Related to Figure 2.

EXTENDED EXPERIMENTAL PROCEDURES

DNA

All Ebolavirus protein sequences are derived from *Ebolavirus Zaire ebolavirus*, strain Mayinga 1976 (EBOV)

Pull-downs

293T cells were grown in DMEM + glucose + 5% fetal bovine serum + 2.5 U/mL penicillin and 2.5 µg/mL streptomycin at 37°C with 5% CO_2. Transfection complexes were formed with 250 ng HA-tagged VP35 or VP35 truncations in the vector pDisplay (Life Technologies) with an equal amount of NP-pcDNA, diluted with 50 µL phosphate buffered saline and finally mixed with 1.5 µL of 1 mg/mL polyethylenamine (Polysciences Inc.). After incubating the complexes at room temperature for 10 minutes, the transfection complexes were added to 80% confluent cells in a 12-well plate. Cells were lysed after two days in 100 µL of 50 mM TrisCl pH 8.0, 300 mM NaCl, 2 mM EDTA, 10% glycerol and 0.1% Igepal CA-630. Lysates were cleared by centrifugation and HA-tagged proteins were bound to 25 µL anti-HA agarose beads (Roche) overnight at 4°C. Beads were washed with three times with 150 µL of lysis buffer. Beads were resuspended and boiled in 30 µL SDS-PAGE sample buffer prior to loading SDS-PAGE gels. The gels were transferred to nitrocellulose for Western blotting. Western blots were blocked in 5% non-fat dry milk and washed with phosphate buffered saline + Tween20. Primary antibodies for Western blotting were anti-HA for VP35 detection (Covance, HA.11 Clone 16B12 mouse monoclonal antibody) or KZ51 for NP detection (Ebola virus disease human survivor monoclonal antibody,(Meissner et al., 2002)). Blots were incubated with appropriate secondary antibodies coupled to horseradish peroxidase and imaged with enhanced chemiluminescent reagent.

Recombinant Protein Expression and purification

Proteins were expressed in *Escherichia coli* using the pET46 vector (Novagen). For co-expression of VP35 and NP, VP35 was cloned in frame with the upstream hexahistidine-tag and the two proteins were expressed from a bi-cistronic mRNA. For preparation of oligomeric NP, an N-terminal MBP fusion was used as a spacer between the 6xHis-tag and the NP. All DNA constructs were validated by Sanger sequencing. Plasmid DNA were transformed into Rosetta2 pLysS *E. coli* (Novagen) and starter cultures were grown with 18 µg/mL chloramphenicol and 100 µg/mL ampicillin in 50 mL Luria-Bertaini broth (LB). Overnight starter cultures were used to inoculate 1 L LB cultures with 100 µg/mL ampicillin. Cultures were induced with a final concentration of 0.5 mM isothiopropyl-galactoside (IPTG) at an optical density at 600 nm of 0.4. Bacteria were allowed to express protein overnight (16-20 hours). Cells were harvested by centrifugation and resuspended in 50 mM TrisCl pH 8.0, 300 mM NaCl, 30 mM imidazole and 2mM BME. Lysis was performed in a Microfluidizer (Microfluidics M110-P). Cell lysates were cleared by centrifugation followed by filtration through a 0.22 µm filter. 5 mL of Ni-NTA Agarose beads were added per liter of culture and incubated at 4°C. Ni-NTA beads were loaded onto a gravity flow column and washed twice with the ten column volumes of the same buffer. His-tagged proteins were eluted from the Ni-NTA with four column volumes of the same buffer containing 300mM imidazole.

In cases where TEV protease was used to cleave the eluted protein, purified TEV protease at 1 mg/mL was added to the Ni-NTA elutions at a final concentration of 0.5% (w/w). This sample was then dialyzed overnight and for some samples, was passed back over Ni-NTA to deplete uncleaved proteins. For purification of the protein by anion exchange chromatography, the protein was dialyzed into 50 mM TrisCl pH 8.5, 100 mM NaCl, 5mM BME before applying the protein to the column. All proteins underwent final purification by size-exclusion chromatography using Superdex200 resin.

Expression of RNA-free NP 1-450 oligomers was accomplished using a construct encoding EBOV VP35 1-80- ENLYFQGSG-NP 1-450 as above which was confirmed to be RNA-free by UV absorbance. Elution fractions from Ni-NTA were dialyzed into 50 mM TrisCl pH 8.5, 100 mM NaCl, 5 mM BME overnight. The monomeric fusion protein was purified by anion exchange chromatography using a 0.6 M NaCl linear gradient. The monomeric protein was then cleaved with 0.5% (w/w) TEV protease overnight and again dialyzed into buffer with 100 mM NaCl. The cleaved fusion protein was re-purified by anion exchange chromatography as above which separated the VP35 1-80 peptide (column flow through) from the NP 1-450 (later elution). The NP 1-450 fractions from anion exchange were finally purified by size-exclusion chromatography where the protein elutes in the void volume of the Superdex 200 column. The UV absorbance was checked at each chromatographic step to ensure that RNA was not introduced from exogenous sources. This was particularly important for size-exclusion chromatography where the oligomeric NP 1-450 was able to bind RNA from dirty columns.

Nucleic acid content was assessed by measuring the A_{260}/A_{280} ratios of the purified proteins. A_{260}/A_{280} ratios less than 0.7 were considered to be RNA-free.

Hydrogen/Deuterium Exchange Mass Spectrometry

To maximize peptide sequence coverage of Ebola virus NP proteins, the optimal quench conditions were established as previously described (Li et al., 2011; Zhang et al., 2012). Briefly, 12 μl of diluted protein stock solution (0.25 mg/ml in 10 mM Tris, 150 mM NaCl, pH 7.2) was mixed with 18 μl of quench buffer (0.8 M, 1.6 M or 3.2 M guanidine HCl in 0.8% formic acid, 16.6% glycerol) on ice and then subjected to proteolysis and LCMS analysis. The use of 1.6 M guanidine HCl resulted in optimal sequence coverage of the proteins. The deuterium exchange experiment was carried out by

mixing 3 µl of protein stock solution with 9 µl of D_2O buffer (8.3 mM Tris, 150 mM NaCl in D_2O, pDread 7.2) and incubating at 0°C for 10, 100 or 1000 sec. The exchange reaction was quenched by adding 18 µl of ice-cold optimal quench solution (1.6 M guanidine HCl, 16.6% Glycerol, 0.8% formic acid), immediately frozen on dry ice, and stored at –80 °C. The un-dueterated control samples and equilibrium-deuterated control samples were also prepared by mixing protein with H_2O buffer (8.3 mM Tris, 150 mM NaCl in D_2O, pH 7.2) and equilibrium-deuterated buffer (0.8% formic acid in 99.9% D_2O) (Sela-Culang et al., 2014). The frozen samples were then thawed at 5 °C and passed over an immobilized pepsin column (16 µl bed volume) at a flow rate of 20 µl/min, and the resulting peptides were collected on a C18 trap for desalting and separated by a Magic C18AQ reverse phase column (Michrom BioResources Inc.) using a linear gradient of acetonitrile from 6.4% to 38.4% over 30 min. MS analysis was performed using OrbiTrap Elite Mass Spectrometer (ThermoFisher Scientific), with a capillary temperature of 200 °C. Data were acquired in both data-dependent MS/MS mode and MS1 profile mode, and the data was analyzed by Proteome Discoverer software and DXMS explorer (Sierra Analytics Inc., Modesto, CA).

Crystallization and Structure Solution

The EBOV VP35 15-60–NP 34-367 was purified by Ni-NTA, MonoQ and Superdex200 chromatography as described above. The protein was concentrated to 10 mg/mL and crystallization proceeded via sitting drop vapor diffusion experiments at 4°C. The $P22_12_1$ crystals grew in 12% PEG 6000, 100 mM MES pH 5.0, using 6.8 mg/mL protein, 0.2 µL protein + 0.2 µL well solution and were cryoprotected in 20% glycerol. The $P2_12_12_1$ crystals grew in 2.0 M sodium formate, 100 mM sodium acetate pH 4.4, using 5.1 mg/mL protein, 0.2 µL protein + 0.2 µL well solution and were cryoprotected in 25% glycerol. The $I2_12_12_1$ crystals grew in 2.2 M sodium formate, 100 mM sodium acetate pH 4.7,

using 14 mg/mL protein, 1.0 µL protein + 1.0 µL well solution and were cryoprotected in 30% glycerol. Cryoprotected crystals were flash-cooled in liquid nitrogen. Data were collected at the Advanced Photon Source at Argonne National Labs, beamlines 23ID-B and 23ID-D. Data were reduced with XDS (Kabsch, 2010) and merged with AIMLESS (Evans, 2011) or XSCALE (Kabsch, 2010). Sulfur phasing was performed in Phenix AutoSol (Adams et al., 2010) for the $I2_12_12_1$ space group with subsequent molecular replacement into $P22_12_1$ and $P2_12_12_1$. Solutions were rebuilt in Coot (Emsley et al., 2010) and refined with Phenix.refine (Adams et al., 2010), BUSTER-TNT (Blanc et al., 2004) with final rounds of refinement in Refmac (Murshudov et al., 2011).

RNA binding assay

Fluorescence anisotropy experiments were set up according to (Rossi and Taylor, 2011). An 18-nucleotide RNA (CGGACACACAAAAAGAAA) corresponding to the 5' positives sense EBOV leader sequence and labeled at its 5' terminus with carboxyfluoscein was purchased from Integrated DNA Technologies. RNA was resuspended at 80 µM in 1 mM TrisCl pH 8.5. All experiments were run in 10 mM $MgCl_2$, 25 mM TrisCl pH 8.0, 150 mM NaCl and 5 mM BME (FP buffer). The RNA was diluted to 80 nM in FP buffer. Protein dialyzed into FP buffer was prepared at 20 µM stock concentrations and serially diluted two-fold 13 times with FP Buffer. 90 µL of each protein dilution was mixed with 5 µL of fluorophore-RNA (final concentration 4 nM) and 5 µL FP buffer. Alternatively, the FP buffer in the final mixture was replaced with a 10 mg/mL solution of Torula yeast type IV (Sigma Aldrich) to assess any non-specific binding of the fluorophore-RNA to the protein. No non-specific binding was observed in any of these samples; hence no subtraction of the binding signal was carried out. Samples were also prepared which contain only the protein dilutions and lacked any RNA to assess the intrinsic sample fluorescence. Fluorescence anisotropy was read on a Tecan

Infinite 200 Pro. The contributions from the protein-only sample to the fluorescence in the parallel and perpendicular directions was subtracted from the corresponding fluorescence of the fluorophore-RNA-containing samples prior to calculating the anisotropy. Reported anisotropies are the average and standard deviations of three replicate experiments.

Mini-genome assay

Screening of VP35 mutants was done as in (Jasenosky et al., 2010). HEK 293T cells were propagated in DMEM + 5% FBS + 25 U/mL streptomycin and 25 µg/mL penicillin. Cells were seeded into 12-well plates and grown to 70% confluency prior to transfection. For the transfection, 2 µg of L-pCAGGS, 0.25 µg VP30-pCAGGS, 0.5 µg T7-pCAGGS, 0.5 µg of 3E5E-T7-Firefly Luciferase, 0.1 µg of Renilla Luciferase-pCAGGS and 0.75 µg of NP-2A-VP35-pCAGGS, where VP35 was either wild-type or mutated in the N-terminal conserved region, were mixed with TransIT-LT1 (Mirus Bio) in a 1:3, DNA:reagent ratio in 100 µL of OPTI-MEM for 20 minutes at room temperature and then added dropwise to cells. Cells were incubated for three days at 37°C with 5% CO_2.

Samples were prepared according to manufacturer's instructures (Promega, Dual Luciferase Assay Kit). Cells were washed with 100 µL PBS and lysed with 100 µL 1X Passive Lysis Buffer. Cells were taken through a freeze/thaw cycle and cleared by centrifugation. Luciferase assays were performed on an Infinite 200 Pro (Tecan) with autoinjectors. 10 µL of cleared lysate was mixed with 50 µL of Luciferase Assay Reagent II, allowed to settle for 2 s and then the signal was integrated for 10 s to measure firefly luciferase acitivity. 50 µL of Stop-and-Glow reagent was then added, allowed to settle for 2 s and integrated for 10 s to measure Renilla luciferase activity. The firefly luciferase activity resulting from the mini Ebola replicon was normalized to the Renilla luciferase which was co-transfected into cells as a transfection control. Data is presented as the percent of the firefly luciferase

assay produced from the mini-genome using wild-type VP35 and represents the result of three replicates.

Electron Microscopy

Copper grids (carbon coated, 400 mesh, Electron Microscopy Sciences, Hatfield PA) were glow discharged and inverted on a 7 µl aliquot of sample for 2 minutes. Excess sample was removed and the grids immediately placed on a droplet 2% uranyl acetate solution for 2 minutes. Excess stain was removed and the grid allowed to dry thoroughly. Grids were then examined on a Philips CM100 electron microscope (FEI, Hillsbrough OR) at 80 kv and images collected using a Megaview III CCD camera (Olympus Soft Imaging Solutions GmbH, Münster, Germany).

SUPPLEMENTAL REFERENCES

Adams, P.D., Afonine, P.V., Bunkoczi, G., Chen, V.B., Davis, I.W., Echols, N., Headd, J.J., Hung, L.W., Kapral, G.J., Grosse-Kunstleve, R.W., *et al.* (2010). PHENIX: a comprehensive Python-based system for macromolecular structure solution. Acta Crystallogr. D Biol. Crystallogr. *66*, 213-221.

Blanc, E., Roversi, P., Vonrhein, C., Flensburg, C., Lea, S.M., and Bricogne, G. (2004). Refinement of severely incomplete structures with maximum likelihood in BUSTER-TNT. Acta Crystallogr. D Biol. Crystallogr. *60*, 2210-2221.

Emsley, P., Lohkamp, B., Scott, W.G., and Cowtan, K. (2010). Features and development of Coot. Acta Crystallogr. D Biol. Crystallogr. *66*, 486-501.

Evans, P.R. (2011). An introduction to data reduction: space-group determination, scaling and intensity statistics. Acta Crystallogr. D Biol. Crystallogr. *67*, 282-292.

Jasenosky, L.D., Neumann, G., and Kawaoka, Y. (2010). Minigenome-based reporter system suitable for high-throughput screening of compounds able to inhibit Ebolavirus replication and/or transcription. Antimicrob. Agents Chemother, *54*, 3007-3010.

Kabsch, W. (2010). XDS. Acta Crystallogr. D Biol. Crystallogr. *66*, 125-132.

Li, S., Tsalkova, T., White, M.A., Mei, F.C., Liu, T., Wang, D., Woods, V.L., Jr., and Cheng, X. (2011). Mechanism of intracellular cAMP sensor Epac2 activation: cAMP-induced conformational changes identified by amide hydrogen/deuterium exchange mass spectrometry (DXMS). J. Biol. Chem. *286*, 17889-17897.

Meissner, F., Maruyama, T., Frentsch, M., Hessell, A.J., Rodriguez, L.L., Geisbert, T.W., Jahrling, P.B., Burton, D.R., and Parren, P.W. (2002). Detection of antibodies against the four subtypes of ebola virus in sera from any species using a novel antibody-phage indicator assay. Virology *300*, 236-243.

Murshudov, G.N., Skubak, P., Lebedev, A.A., Pannu, N.S., Steiner, R.A., Nicholls, R.A., Winn, M.D., Long, F., and Vagin, A.A. (2011). REFMAC5 for the refinement of macromolecular crystal structures. Acta Crystallogr. D Biol. Crystallogr. *67*, 355-367.

Rossi, A.M., and Taylor, C.W. (2011). Analysis of protein-ligand interactions by fluorescence polarization. Nat. Protoc. *6*, 365-387.

Sela-Culang, I., Benhnia, M.R., Matho, M.H., Kaever, T., Maybeno, M., Schlossman, A., Nimrod, G., Li, S., Xiang, Y., Zajonc, D., *et al.* (2014). Using a combined computational-experimental approach to predict antibody-specific B cell epitopes. Structure *22*, 646-657.

Zhang, A.P., Bornholdt, Z.A., Liu, T., Abelson, D.M., Lee, D.E., Li, S., Woods, V.L., Jr., and Saphire, E.O. (2012). The ebola virus interferon antagonist VP24 directly binds STAT1 and has a novel, pyramidal fold. PLoS Pathog. *8*, e1002550.